

Synthesis, characterization, and morphological control of PbWO₄ nanostructures through precipitation method and its photocatalyst application

Saeid Pourmasoud¹ · Mohammad Eghbali-Arani¹ · Farhad Ahmadi² · Mehdi Rahimi-Nasrabadi³ 

Received: 19 June 2017 / Accepted: 1 August 2017 / Published online: 7 August 2017
© Springer Science+Business Media, LLC 2017

Abstract In current study, we synthesized PbWO₄ using co-precipitation method. Also the effect of three capping agents, polyethylene glycol, cetyltrimethylammonium and sodium dodecyl sulfate on the size of particles, morphology, and photocatalytic properties of nano-structures was investigated. The techniques we employed to characterize the morphological, optical, magnetic and structural properties of as-obtained products were, scanning electron microscopy, vibrating sample magnetometer, energy dispersive X-ray, UV–Vis spectroscopy and X-ray diffraction. The methyl orange method was utilized to assess photocatalytic activity of as-obtained nano-particles under ultraviolet (UV) radiation. Our findings validated that PbWO₄ can be decolorized up to maximum value of 97% under 90 min UV irradiation.

1 Introduction

Supplying fresh water, nowadays, has turned into one of the biggest challenges which all countries, needless to say, they are developed or developing, are facing with. Water scarcity problem can stem from many reasons including, earth's rising population, overused of water, climate change and increased pollution [1–5]. The importance of free-toxic

chemical and diseases-producing microorganism water for human health, has caused many scientists to conduct extensive research to pure water using nano technology. Making use of low dimensional nano particles in water purification, due to their extensive application in different aspects, inspired researchers to give much attention to nano structures [6–10].

One of the most significant aspects of metal nanoparticles, is how pollutants can be removed from environment and water. In other words, making use of photocatalytic and solar energy of nanoparticles, this method has been of advantage to value and efficiency. Changing of living components to carbon dioxide and water without making of remarkable amount of toxics is beneficially of utmost importance [11, 12]. Due to photocatalytic degradation of natural structures, Wolframite-type tungstates of transition metals (MWO₄, M=Iron, Cadmium, Zinc, Nickel, Cobalt, rare earth element) have currently received much attention. The materials are widely utilized as, magnetic materials multiferroics, photovoltaic, scintillator, optical fibers, photoluminescence, super capacitors, scintillators, molecular precursors to metal tungstate, photocatalyst, and etc [13–15]. The previous studies have demonstrated that tungsten oxide (WO₃) can be considered as an active photocatalyst material for oxygen evolution, whereas, its activity for hydrogen evolution has not still been proved. That is why different efforts have been made to achieve a series of materials in which MWO₃ and MWO₄ would be considered as strong photocatalyst compounds. Therefore, the obtained materials displayed attractive technological characteristics for example, ferro elasticity, ionic photoluminescence and ferro elasticity [16–19]. But to synthesize MWO₄, one may perform various methods, such as solid state reaction, solution combustion, sol–gel, solvothermal synthesis, co-precipitation, and

✉ Mehdi Rahimi-Nasrabadi
Rahiminasrabadi@gmail.com

¹ Department of Physics, University of Kashan, Kashan, Iran

² Department of Medicinal Chemistry, School of Pharmacy-International Campus, University of Medical Sciences, Tehran, Iran

³ Faculty of Pharmacy, Baqiyatallah University of Medical Sciences, Tehran, Iran

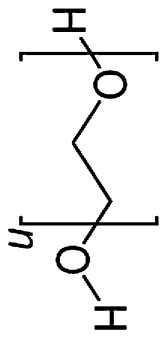
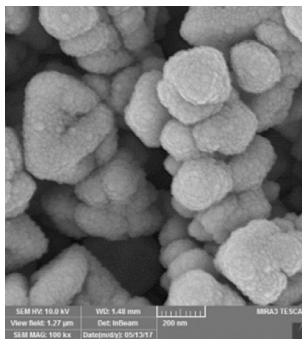
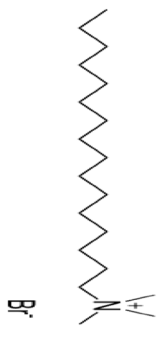
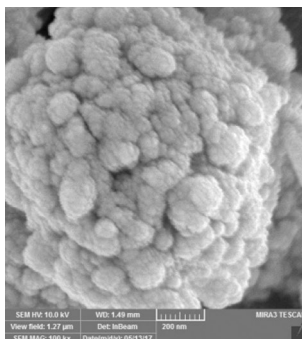
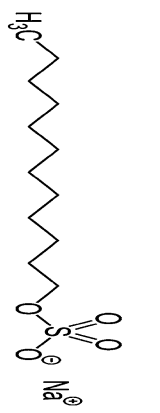
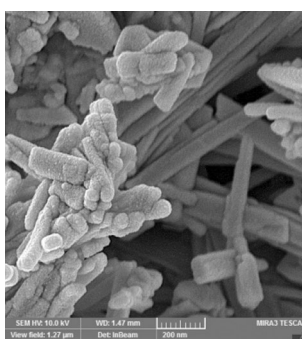
hydrothermal synthesis [20–23]. Of procedures already mentioned, one can expect that co-precipitation method is more advantageous, due to its more simplicity, cost effectiveness, softness chemical synthetic methodology, and fastness in comparison with the rest methods. Also, co-precipitation method does not need specific working conditions, and high temperature to be calcined [24–28]. Therefore, these advantages motivated us to synthesize PbWO_4 nanoparticles based on co-precipitation. The synthesizing has been done in distilled water as solvent. In addition, polyethylene glycol, cetyltrimethylammonium and sodium dodecyl sulfate as capping agents, were employed to obtain their influence on the size of particles and morphology of founded nanoparticles.

2 Experimental

2.1 Synthesis of PbWO_4 nanostructures

A new simplistic co-precipitation method was employed to prepare nanocrystalline lead tungstate. We followed a step-by-step procedure to make lead tungstate. Firstly, we dissolved 1 mmol of $\text{Na}_2\text{WO}_4 \cdot 2\text{H}_2\text{O}$ in hot water (typically 70°C). Secondly, it was added drop-by-drop to a 20 ml hot solution (50°C) containing 1 mmol of $\text{Pb}(\text{NO}_3)_2$ and 3 mmol surfactants with magnetic stirring. We regulated the pH of gained solution in 5–6. Afterwards, under constant magnetic stirring, the resultant solution was heated at 90°C for 1 h, and then we permitted the system to cool

Table 1 Preparation conditions for the synthesis of PbWO_4 nanoparticles

Sample no	Surfactant	Solvent	Decolorization (%)	Surfactant figure	SEM
1	PEG	Water	97		
2	CTAB	Water	95		
3	SDS	Water	84		

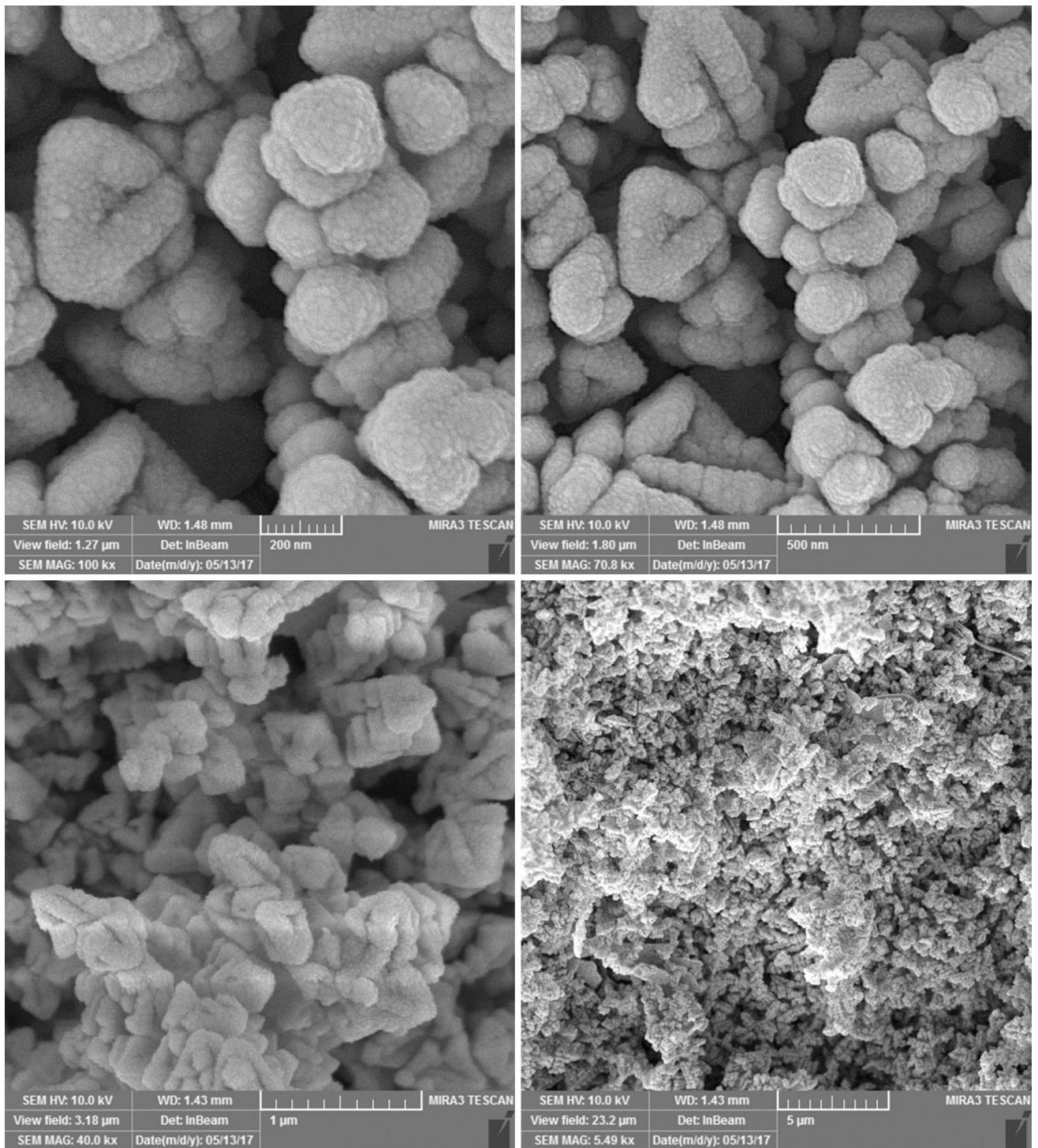


Fig. 1 SEM images of PbWO₄ nanoparticles with PEG (sample 1)

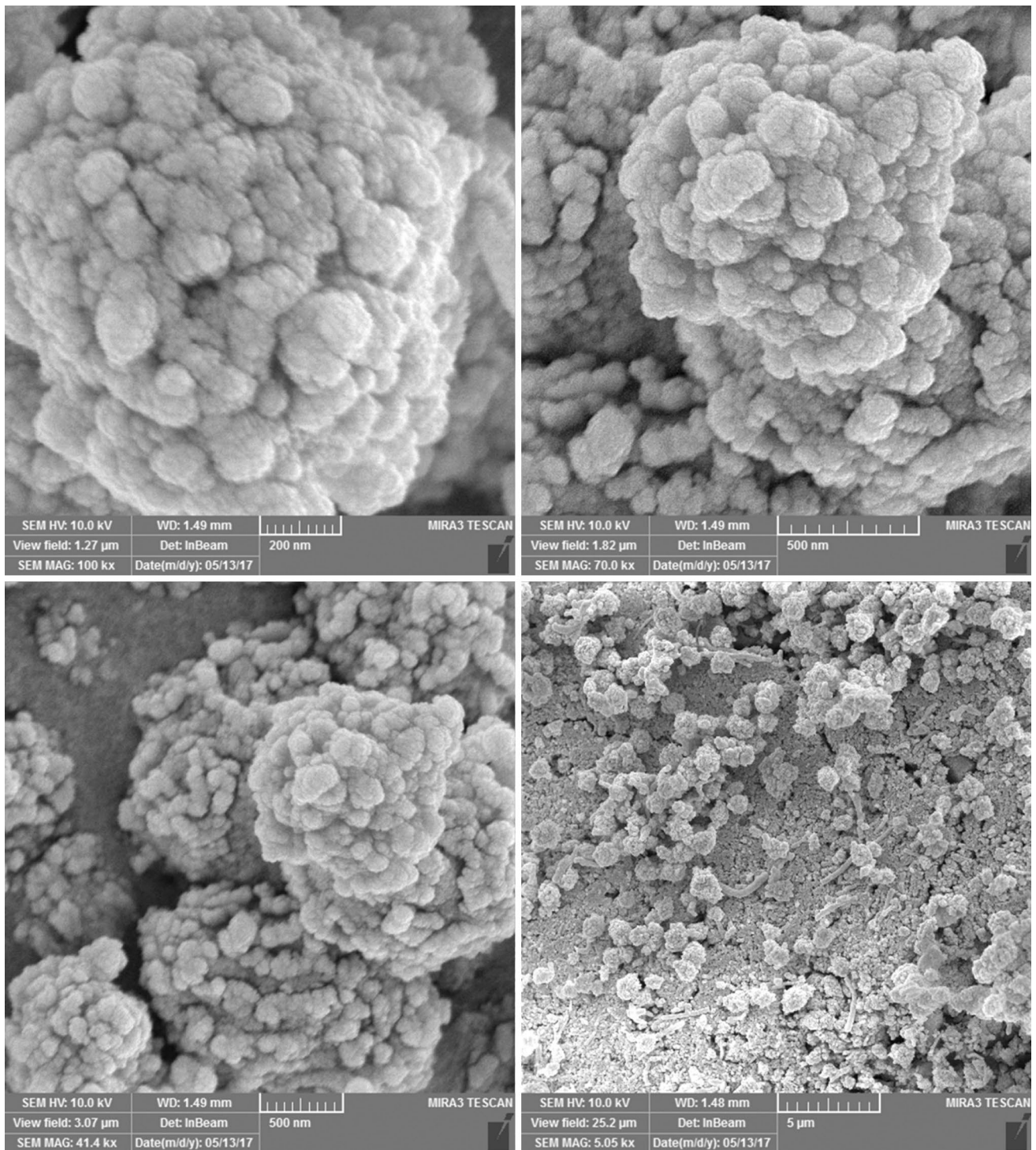


Fig. 2 SEM images of PbWO₄ nanoparticles with CTAB (sample 2)

to normal temperature. Subsequently, we collected the obtained precipitation by filtration, and washed several times with absolute ethanol and distilled water. Finally, we dried the product in vacuum at 90 °C. Reaction conditions are available in Table 1.

2.2 Photocatalytic test

To perform photocatalytic activity of PbWO_4 nanoparticles, we monitored the degradation process in a quartz photocatalytic reactor when they were exposed to ultraviolet radiation. Firstly, we mixed 0.1 g of nanoparticles with 50 ppm solution of dyes to carry out Photocatalytic degradation. Afterwards, the mixture was positioned in photoreactor under UV light and stirred for half hour at dark, ensuring proper adsorption–desorption equilibrium of the dye molecules on the surface of nanostructures requiring to operate as a photocatalyst efficiently. Then, air was blown into the vessel via a pump maintaining the solution oxygen-saturated for the duration of the reaction. Eventually, the separation of PbWO_4 was done from the 5 ml samples and removed from the degraded solution at different time intervals, making use of 10 min centrifuging at 10,000 rpm. A UV–Vis spectrophotometer was used to obtain dye concentration.

2.3 Characterization

The cetyltrimethylammonium bromide (CTAB), polyethylene glycol (PEG), and sodium dodecyl sulfate (SDS) and lead nitrate ($\text{Pb}(\text{NO}_3)_2$), sodium tungstate ($\text{Na}_2\text{WO}_4 \cdot 2\text{H}_2\text{O}$), were prepared from a well known company, Merck. X-ray diffraction spectra (XRD) were recorded on a Philips-X'PertPro instrument with a Ni-filtered $\text{Cu K}\alpha$ radiation at a scan range of $10 < 2\theta < 80$. The scanning electron microscopy (SEM) studies were performed on a LEO-1455VP with an energy dispersive X-ray spectroscope. An S-10 4100 Scinco UV–Vis scanning spectrometer was utilized to gain the electronic spectra. Energy dispersive spectra (EDS) were also acquired making use of an XL30 Philips microscope and the magnetic measurements were performed using a vibrating sample magnetometer (VSM) (Meghnatis Daghigh Kavir Co.; Kashan Kavir; Iran) under ambient temperatures.

3 Results and discussion

In the few past years through the control of reaction parameters, particle size and control of shape of nanostructures has absorbed much attentiveness. Owing to high dependency of nanoparticles on their shape and particle size [29–34], several experiments were carried out to explore

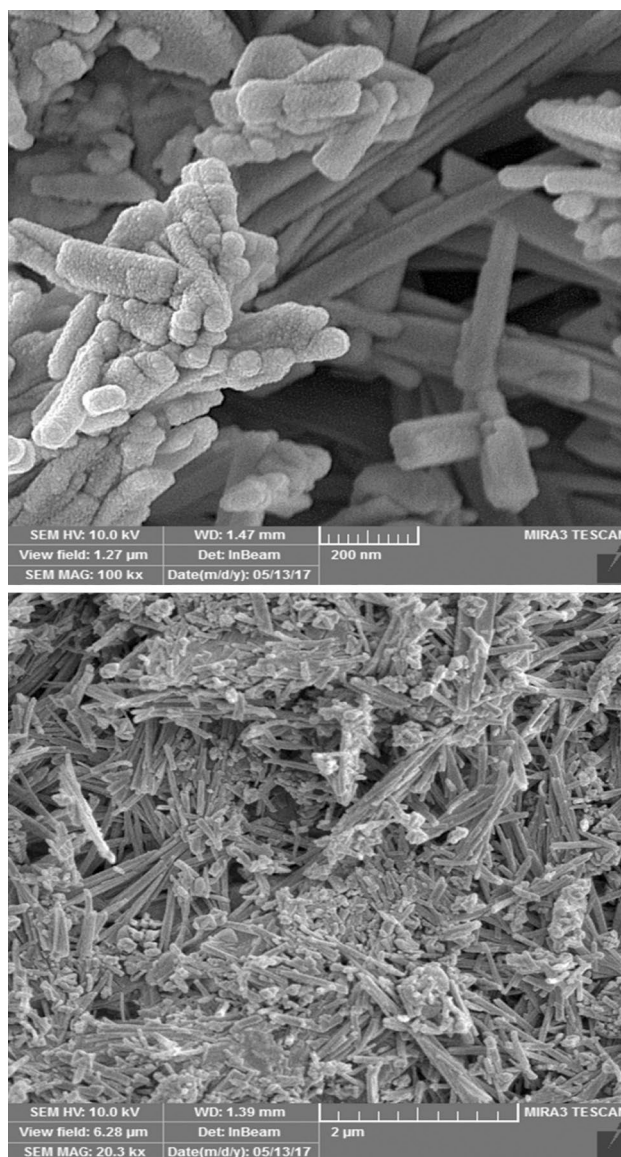


Fig. 3 SEM images of PbWO_4 nanoparticles with SDS (sample 3)

the effect of different surfactants on the particle size and morphology of PbWO_4 nanoparticles. Using SEM images, we explained the morphologies. Figures 1, 2, and 3 make clear the SEM images of PbWO_4 nanoparticles, which were prepared by CTAB, PEG, and SDS as various capping agents in agreement with sample 1, 2 and 3, respectively.

The effect of presence of PEG, as a polymeric surfactant, on the morphology of synthesized PbWO_4 nanoparticles at low temperature, is given in Fig. 1. The SEM images clarified that they are in triangle-like shape and are consist of nanostructures with the average size of 40 nm. The coalesced image of PbWO_4 with the average size of 80 nm in the presence of CTAB as a cationic surfactant and rod-like PbWO_4 nanoparticles with the average length of 60 nm

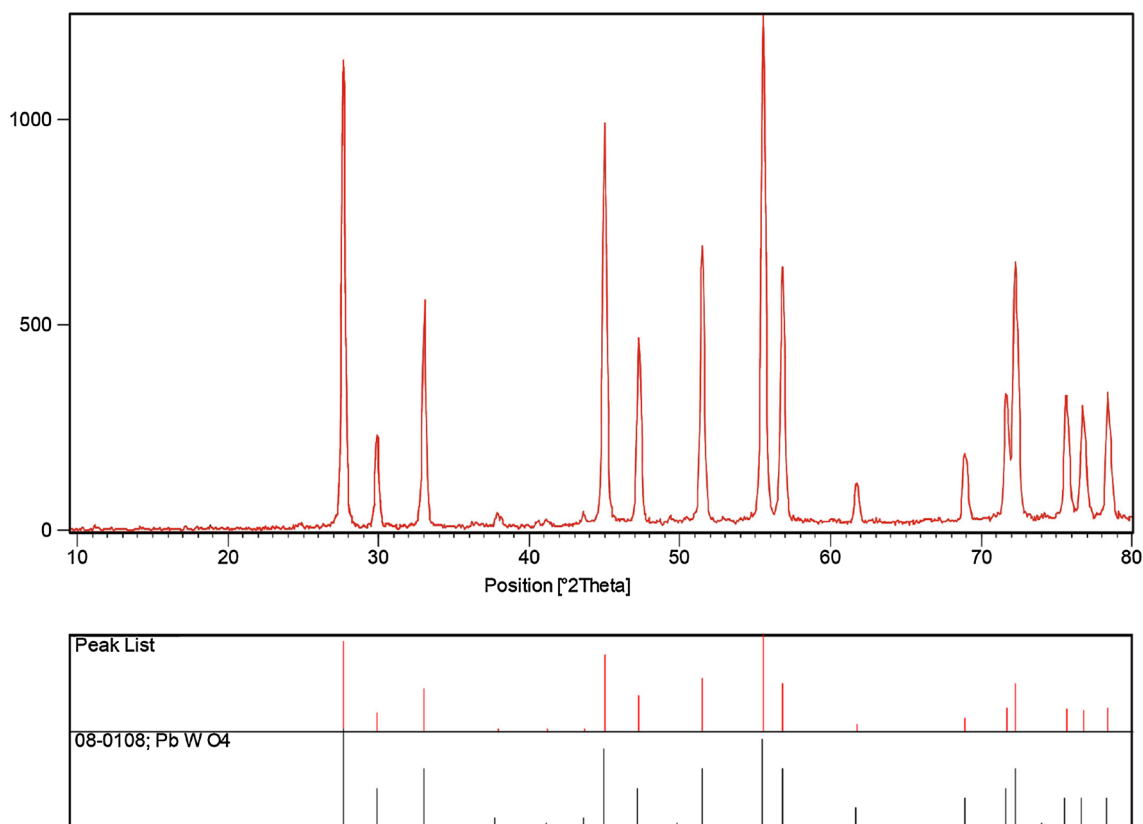


Fig. 4 XRD pattern of PbWO₄ nanoparticles (sample 1)

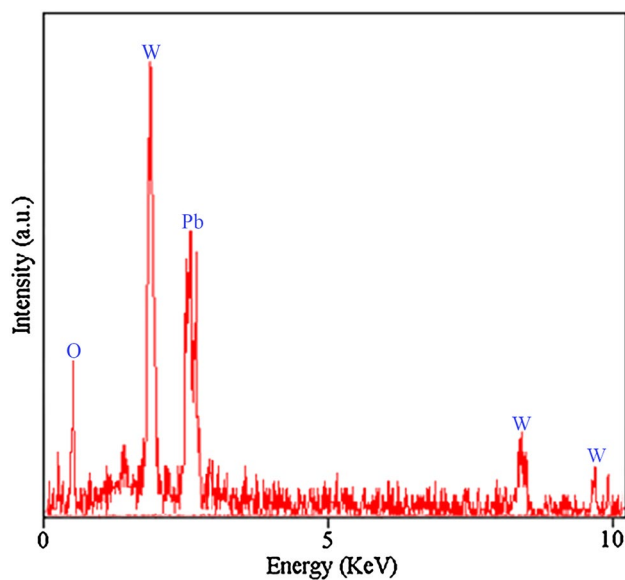


Fig. 5 EDS pattern of PbWO₄ nanoparticles (sample 1)

and width of 2 μm due to using SDS as anionic surfactant have been shown in Figs. 2 and 3 respectively. In addition, because of spatial configuration of SDS surfactant, the

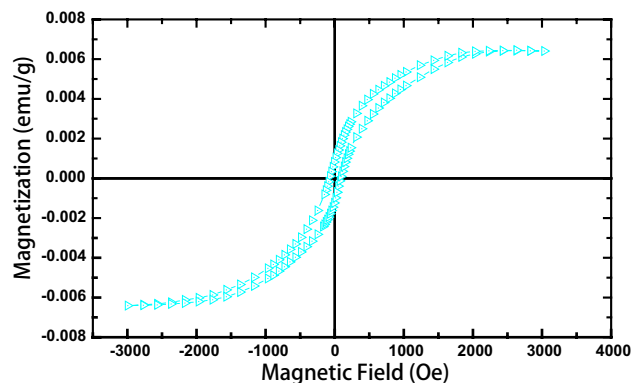


Fig. 6 VSM curves of PbWO₄ nanoparticles (sample 1)

morphology of PbWO₄ nanoparticles are also in the rod-like shape.

In Fig. 4 XRD, the pattern of PbWO₄ nanoparticles has been displayed. In addition, the XRD demonstrated the presence of both tetragonal phase of PbWO₄ nanoparticles (JCPDS No. 08-0108, space group: I41/a). The formation of impurity-free PbWO₄ nanoparticles, also proved by XRD pattern. The size of crystalline is computed from Scherrer formula as the following:

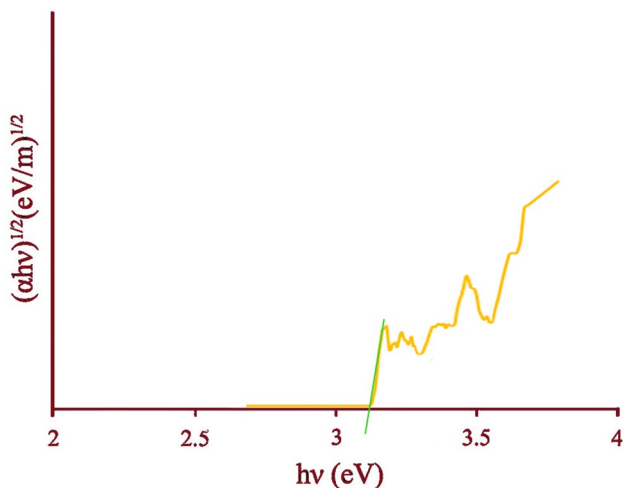


Fig. 7 DRS pattern of PbWO₄ nanoparticles (sample 1)

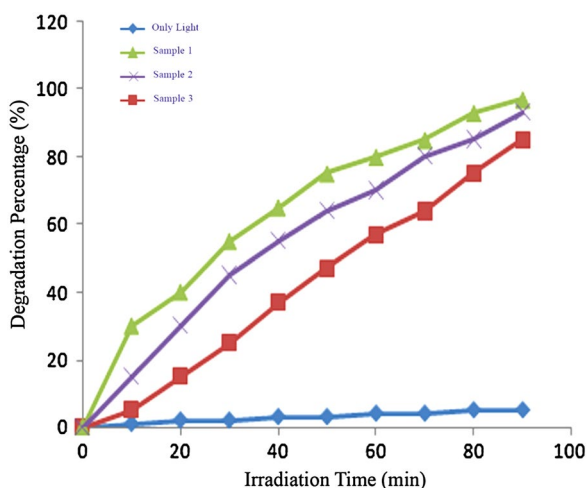


Fig. 8 Photocatalytic methyl orange degradation of PbWO₄ nanoparticles under ultraviolet light

$$D_c = K\lambda/\beta\cos\theta, \tag{1}$$

where β , K and λ are the width of the observed diffraction peak at its half maximum intensity (FWHM), the shape factor which takes a value of about 0.9 and the X-ray wavelength (Cu K α radiation, equals to 0.154 nm) were about 11 nm for PbWO₄ nanoparticles respectively. The analysis of EDS showed the presence of O, Pb and W elements without any impurity (Fig. 5). The measurements of magnetization as a function of the magnetic field were investigated at 300 K, and the hysteric curve with nearly saturated nature at high fields is represented in Fig. 6. Our findings in relation to magnetic properties of PbWO₄ nanoparticles, showed that, there magnetic contribution of PbWO₄

nanoparticles is small at room temperature. Additionally, the analysis of VSM uncovered that PbWO₄ nanoparticles has ferromagnetic properties. The coercivity and saturation magnetization are found to be 80 Orsted and 0.006 emu g⁻¹ and respectively.

Commonly, the band-gap of the nanostructures materials has a major role to play to use photocatalytic applications. The diffuse reflectance spectroscopy (DRS) for PbWO₄ nanoparticles has been illustrated in Fig. 7. The band-gap of the samples was measured by the following equation:

$$(\alpha hv)^n = (hv - E_g) \tag{2}$$

where, B , α , E_g , $h\nu$, and n are material constant, the amount of the absorbance, the optical band gap of the material, the photon energy, and a constant that depends on the type of the electronic transition respectively. Using extrapolating the linear portion of the plots of $(\alpha hv)^2$ curve in return $h\nu$ to the energy axis, the energy gap of the samples (E_g) was found. The value of band-gap (E_g) for PbWO₄ nanoparticles was 3.2. To investigate the photocatalytic activity, PbWO₄ nanoparticles were used. The photocatalytic efficiency was evaluated by the following Eq. (3):

$$\text{Color removal (\%)} = (C_0 - C_t / C_0) \times 100 \tag{3}$$

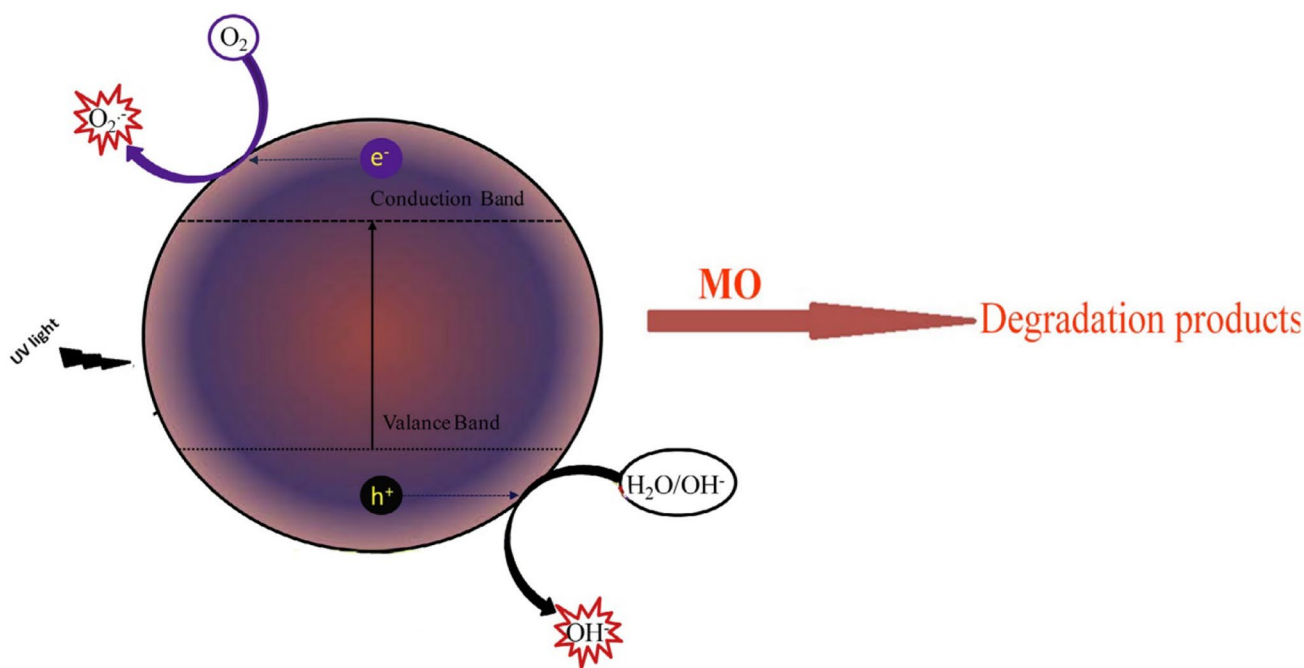
where (mg L⁻¹) is the concentration of MO at any irradiation time t (min) and C_0 (mg L⁻¹) is the initial concentration of MO in solution. In Fig. 8 we have shown that, for MO, after 90 min, the degradation rate of PbWO₄ nanoparticles was 97, 95, and 84% for PEG, CTAB, and SDS respectively. Therefore, we could find to smallness of recombination of electron–hole possibility in PbWO₄ nanoparticles, causing holes in valance band react with OH groups on the surface of nanoparticles. This can turn them into highly reactive OH \cdot radicals. The reaction of produced radicals with MO and its degradation has come in Scheme 1. According to the Langmuir–Hinshelwood kinetics model, the kinetics of the photocatalytic decolourization rate of MO was acquired. This is given in the following Eq. (4):

$$\ln(C_0/C_t) = k_{app}t \tag{4}$$

Utilizing the slope of $\ln(C_0/C_t)$ in terms of irradiation time t , we quantified. The pseudo-first-order rate constant, k_{app} (min⁻¹) [35–38].

4 Conclusions

The removal of MeO dyes from water was done by preparation of PbWO₄ nanoparticles. The co-precipitation method was employed to synthesize PbWO₄ nanoparticles effectually. The influence of preparation three various surfactants such as PEG, CTAB and SDS on morphology and particle



Scheme 1 Reaction mechanism of methyl orange photodegradation over PbWO_4 nanoparticles under UV light irradiation

size of products were examined. The homogenous synthesizing of PbWO_4 nanoparticles was done, without further impurity. Furthermore, the photocatalytic properties of PbWO_4 nanoparticles arise from the value of its band gap. The investigation of the photocatalytic properties of this product was performed by photo-oxidation of methyl orange (MO). The photocatalytic test affirms that the degradation rate of methyl orange, after 90 min irradiation of UV light, picked at approximately 97% for PEG surfactant.

Acknowledgements Authors are grateful to council of University of Kashan for providing financial support to undertake this work. This work was supported by Council of University of Kashan by Grant Agreement No. 682151/1.

References

- M. Rahimi-Nasrabadi, F. Ahmadi, A. Fosooni, *J. Mater. Sci. Mater. Electron.* **28**, 537 (2017)
- F. Ahmadi, M. Rahimi-Nasrabadi, M. Behpour, *J. Mater. Sci. Mater. Electron.* **28**, 1531 (2017)
- M. Salavati-Niasari, F. Soofivand, A. Sobhani-Nasab, M. Shakhouri-Arani, M. Hamadani, S. Bagheri, *J. Mater. Sci. Mater. Electron.* (2017). doi:10.1007/s10854-017-7369-5
- S.M. Hosseinpour-Mashkani, A. Sobhani-Nasab, *J. Mater. Sci. Mater. Electron.* **27**, 7548 (2016)
- S.M. Hosseinpour-Mashkani, A. Sobhani-Nasab, *J. Mater. Sci. Mater. Electron.* **28**, 4345 (2017)
- F. Ahmadi, M. Rahimi-Nasrabadi, A. Fosooni, M. Daneshmand, *J. Mater. Sci. Mater. Electron.* **27**, 9514 (2016)
- A. Sobhani-Nasab, Z. Zahraei, M. Akbari, M. Maddahfar, S.M. Hosseinpour-Mashkani, *J. Mol. Struct.* **1139**, 430 (2017)
- M. Rahimi-Nasrabadi, *J. Mater. Sci. Mater. Electron.* **28**, 2200 (2017)
- M. Rahimi-Nasrabadi, F. Ahmadi, M. Eghbali-Arani, *J. Mater. Sci. Mater. Electron.* **28**, 2415–2420 (2017)
- M. Rahimi-Nasrabadi, F. Ahmadi, M. Eghbali-Arani, *J. Mater. Sci. Mater. Electron.* **27**, 13294 (2016)
- M. Pirhashemi, A. Habibi-Yangjeh, *J. Colloid Interface Sci.* **491**, 216 (2017)
- A. Habibi-Yangjeh, M. Shekofteh-Gohari, *Sep. Purif. Technol.* **184**, 334 (2017)
- S. Thongtem, S. Wannapop, T. Thongtem, *Ceram. Int.* **35**, 2087 (2009)
- C. Wei, Y. Huang, X. Zhang, X. Chen, J. Yan, *Electrochim. Acta*, **220**, 156 (2016)
- X.C. Song, E. Yang, R. Ma, H.F. Chen, Y. Zhao, *J. Nanopart. Res.* **10**, 709 (2008)
- L. Zhen, W.S. Wang, C.Y. Xu, W.Z. Shao, L.C. Qin, *Mater. Lett.* **62**, 1740 (2008)
- M. Rahimi-Nasrabadi, S.M. Pourmortazavi, M.R. Ganjali, A.R. Banan, F. Ahmadi, *J. Mol. Struct.* **1074**, 85 (2014)
- K. Adib, M. Rahimi-Nasrabadi, Z. Rezvani, S.M. Pourmortazavi, F. Ahmadi, H.R. Naderi, M.R. Ganjali, *J. Mater. Sci. Mater. Electron.* **27**, 4541 (2016)
- W.B. Hu, X.L. Nie, Y.Zh. Mi, *Mater. Charact.* **61**, 85 (2010)
- Z. Lou, J. Hao, M. Covivera, *J. Lumin.* **99**, 349 (2002)
- M. Bonanni, L. Spanhel, M. Lerch, E. Fuglejn, G. Muller, F. Jermann, *Chem. Mater.* **10**, 304 (1998)
- A.R. Phani, M. Passacantando, L. Lozzi, S. Santucci, *J. Mater. Sci. Mater. Electron.* **35**, 4879 (2000)
- F.S. Wen, X. Zhao, H. Huo, J.S. Chen, E. Shu-Lin, J.H. Zhang, *Mater. Lett.* **55**, 152 (2002)
- M. Rahimi-Nasrabadi, *J. Mater. Sci. Mater. Electron.* **28**, 6373 (2017)

25. M. Rahimi-Nasrabadi, M. Behpour, A. Sobhani-Nasab, M. RangrazJeddy, J. Mater. Sci. Mater. Electron. **27**, 11691 (2016)
26. A. Sobhani-Nasab, H. Naderi, M. Rahimi-Nasrabadi, M.R. Ganjali, J. Mater. Sci. Mater. Electron. **28**, 8588 (2017)
27. M. Rahimi-Nasrabadi, H.R. Naderi, M. Sadeghpour Karimi, F. Ahmadi, S. M. Pourmortazavi, J. Mater. Sci. Mater. Electron. **28**, 1877 (2017)
28. S.M. Hosseinpour-Mashkani, M. Maddahfar, A. Sobhani-Nasab. S. Afr. J. Chem. **70**, 44–48 (2017)
29. M. Ramezani, A. Sobhani-Nasab, A. Davoodi, J. Mater. Sci. Mater. Electron. **26**, 5440 (2015)
30. M. Rahimi-Nasrabadi, S.M. Pourmortazavi, M. Khalilian-Shalamzari, J. Mol. Struct. **1083**, 229–235 (2015)
31. M. Rahimi-Nasrabadi, S.M. Pourmortazavi, M.R. Ganjali, P. Novrouzi, F. Faridbod, M. SadeghpourKarimi, J. Mater. Sci. Mater. Electron. **28**, 3325 (2017)
32. M. Rahimi-Nasrabadi, M. Behpour, A. Sobhani-Nasab, S.M. Hosseinpour-Mashkani, J. Mater. Sci. Mater. Electron. **26**, 9776 (2015)
33. H. Reza Naderi, A. Sobhani-Nasab, M. Rahimi-Nasrabadi, M.R. Ganjali, Appl. Surf. Sci. **423**, 1025 (2017)
34. A. Sobhani-Nasab, S.M. Hosseinpour-Mashkani, M. Salavati-Niasari, S. Bagheri, J. ClustSci. **26**:1305–1318 (2015)
35. A. Sobhani-Nasab, M. Rangraz-Jeddy, A. Avanes, M. Salavati-Niasari, J. Mater. Sci. Mater. Electron. **26**, 9552 (2015)
36. A. Javidan, M. Ramezani, A. Sobhani-Nasab, S.M. Hosseinpour-Mashkani, J. Mater. Sci. Mater. Electron. **26**(6), 3813–3818 (2015)
37. M. Akbari, A. Aetemady, F. Firoozeh, M. Yaseliani, J. Mater. Sci. Mater. Electron. **28**, 10245 (2017)
38. M. Ramezani, A. Sobhani-Nasab, S.M. Hosseinpour-Mashkani, J. Mater. Sci. Mater. Electron. **26**(7), 4848 (2015)